Optics and Lasers in Engineering 49 (2011) 1012–1018

Contents lists available at ScienceDirect

Optics and Lasers in Engineering

journal homepage: www.elsevier.com/locate/optlaseng

Application of least-square estimation in white-light scanning interferometry

S. Ma [a,b], C. Quan [b], R. Zhu [a,*], C.J. Tay [b], L. Chen [a], Z. Gao [a]

[a] School of Electronic and Optical Engineering, Nanjing University of Science and Technology, Xiao Lingwei Road 200, Nanjing, Jiangsu 210094, China
[b] Department of Mechanical Engineering, National University of Singapore, 9 Engineering Drive 1, Singapore 117576, Singapore

ARTICLE INFO

Article history:
Received 24 November 2010
Accepted 17 January 2011
Available online 21 February 2011

Keywords:
White-light scanning interferometry (WLSI)
Complex phasor (CP)
Short-time Fourier transform (STFT)
Least-square estimation

ABSTRACT

White-light scanning interferometry (WLSI) is a powerful tool for investigating the profile of a test object that contains sharp steps. Due to the light source used in WLSI system, it is able to overcome phase ambiguity problem, which is often encountered in monochromatic interferometry. In this paper, a new algorithm based on least-square estimation using short-time Fourier transform (STFT) is proposed to measure the profile of a test object. STFT is used to extract the peak position of the coherence envelope of a white-light interference signal and retrieve the corresponding phase values simultaneously at first. A complex phasor (CP) method is introduced to further reduce the phase noise. Then, the phase values at several positions around are utilized to achieve a more accurate peak position based on least-square line fitting. Both simulated and experimental results show that the proposed algorithm is able to accurately measure the profile of a test object.

1. Introduction

As a non-contact technique, optical interferometry has the advantages of high-resolution, fast processing speed and being whole-field for measuring surface profiles [1–3]. However, when the light source is a monochromatic light, owing to the phase ambiguity, the dynamic depth range of measurement is often restricted. Hence, monochromatic interferometry is usually applied only to objects with smooth profile. However in white-light scanning interferometry (WLSI), due to the fact that the white-light source has a very short coherence length, it does not encounter such a problem. The white-light interference signal occurs only when the optical path difference (OPD) between the objective and reference beams is within the coherence length. Hence, the profile of a test object can be determined with high accuracy.

To date, numerous works have been carried out on white-light scanning interferometry (WLSI). These methods are based on Michelson, Linnik, and Mirau interferometers [4–7]. Kino and Chim [8] proposed an algorithm based on Fourier transform to extract the coherence envelope of a white-light interference signal. They first processed the signal with Fourier transform to obtain its spectrum. The positive first order lobe is then extracted using a filtering window and centralized in frequency domain. The absolute values of the inversed Fourier transformed first order side lobe gives the coherence envelope of the original white-light interference signal. Finally, the zero OPD position is determined by a peak position of the extracted envelope. In 1992, Hilbert transform was introduced to extract the coherence envelope by Chim and Kino [9]. However, the accuracy of these two methods depends on their filtering operation. Park and Kim [10] subsequently presented a new method for fringe peak extraction using a direct quadratic polynomial fitting to improve its accuracy. The envelope peak is preliminarily estimated by fitting sampled intensity data directly to a symmetric quadratic polynomial. A more precise fringe peak is determined by compensating for the phase shift on reflection using the absolute fringe order identified by the envelope peak obtained. In order to obtain an accurate peak position, Chen et al. [11] calculated the gravity of coherence envelope. However, this method, possessing a fast processing speed, is only applicable to symmetric signals. Moreover, Sandoz [12] introduced a seven-step phase-shifting algorithm to process the white-light interference signal. The method accurately estimated a zero OPD position using the phase value of the maximum fringe contrast position for compensation. Larkin [13] also described an efficient nonlinear algorithm for more precise envelope detection, which is derived from a five-step phase-shifting algorithm. Harasaki et al. [14] proposed a method that combines phase-shifting and coherence-peak-sensing techniques to permit measurement with a larger dynamic range and remove the bat-wing effect. While, Rolf-Jürgen and Gunther [15] and Li et al. [16] described two different algorithms based on continuous wavelet transform (CWT) to accomplish profile

* Corresponding author.
E-mail address: zhurihong@vip.sina.com (R. Zhu).

0143-8166/$ - see front matter © 2011 Elsevier Ltd. All rights reserved.
doi:10.1016/j.optlaseng.2011.01.013

measurement. These algorithms using Morlet wavelet as the mother wavelet are able to eliminate noise with little distortion of the original signals. In 2008, Sarac [17] used Stockwell transform, which is actually an extension of the CWT to process white-light interference signal. Correspondingly, Groot and Deck [18–21] analyzed the signal in spatial-frequency domain (SFD) and developed a series of algorithms, which utilize the relationship between phase and wave number to accurately locate the zero OPD position. The SFD method has the advantage of requiring fewer limits on the scanning device than other methods and the spectrum of a used light source can asymmetrically distribute.

As an effective kind of tools for time–frequency analysis, short-time Fourier transform (STFT) has been used in several optical testing fields with good results [22–27]. Comparing with the global transform (e.g. Fourier transform), due to its characteristic of local transformation, the poor data points of signal have no effect on others outside the window size of STFT. In this paper, a new algorithm based on least-square estimation using STFT is proposed to measure the profile of a test object in WLSI. STFT is used to extract the peak position of the coherence envelope of a white-light interference signal and retrieve the corresponding phase values simultaneously at first. A complex phasor (CP) method is introduced to further reduce the phase noise. Then, the phase values at several positions around are utilized to achieve a more accurate peak position based on least-square line fitting.

2. Theoretical analysis

2.1. Direct peak detection

In white-light scanning interferometry, the intensity function of an arbitrary point on a test object recorded by a CCD camera along the scanning direction is given by [13]

$$I(z) = I_0 + \gamma I_0 g(z - z_0)\cos[2k_0(z - z_0) + \varphi_0] \quad (1)$$

where I_0 is the background intensity, γ is the fringe contrast, $g(z-z_0)$ is the coherence envelope, which depends on the spectrum of the light source [6,7], z is the vertical scanning position along the optical axis, z_0 is the peak position of the coherence

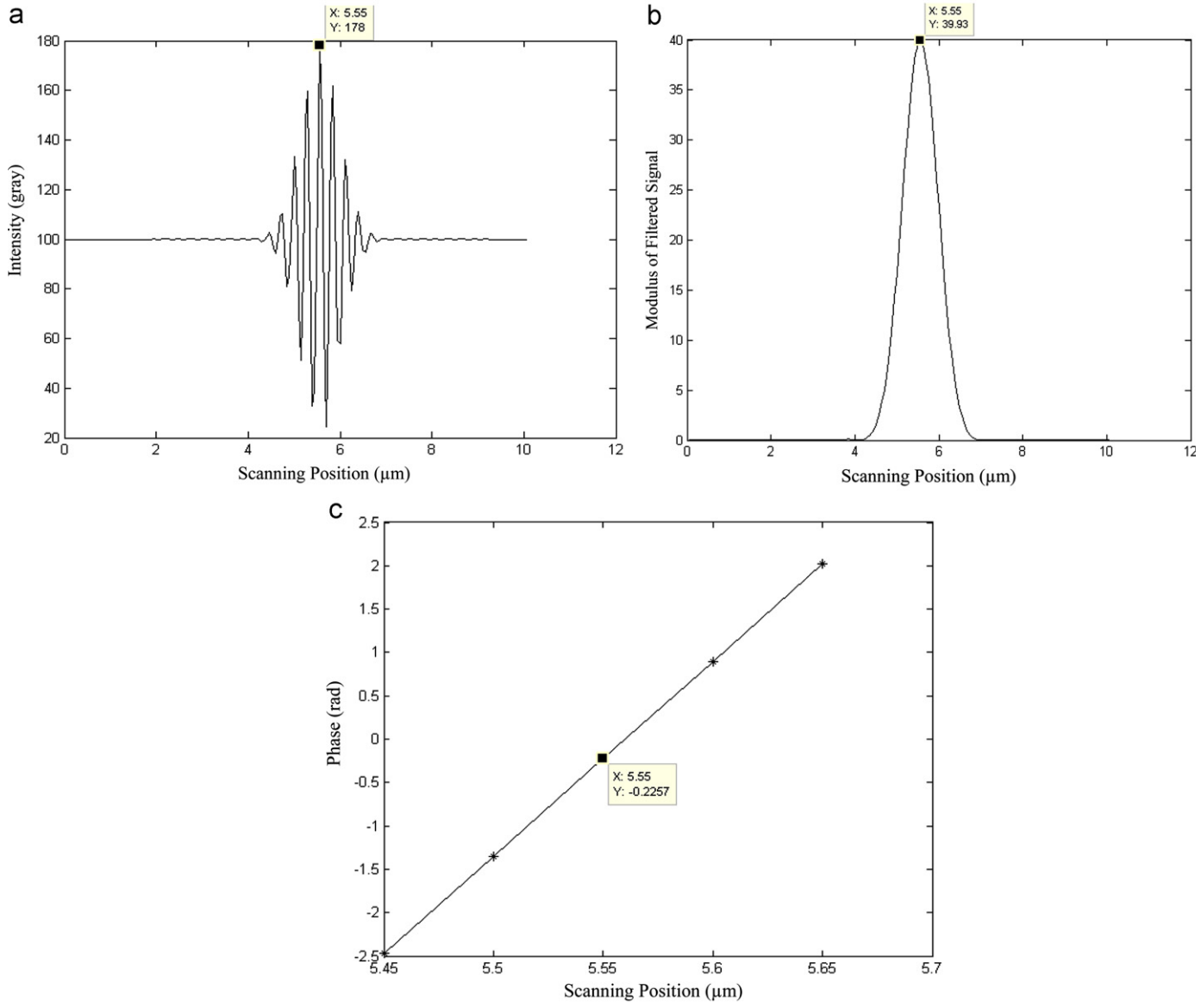

Fig. 1. (a) A simulated white-light interference signal. (b) Modulus of a filtered signal. (c) Least-square estimation using phase values at five points.

envelope, k_0 is the center wave number of the light source, and φ_0 is a phase offset. In this paper, a halogen light source with a Gaussian spectrum is used, and hence the intensity function can be rewritten as

$$I(z) = I_0 + \gamma I_0 \exp\left[-\left(\frac{z-z_0}{l_c}\right)^2\right]\cos\left(\frac{4\pi}{\lambda_0}(z-z_0)+\varphi_0\right) \quad (2)$$

where $l_c = (c\sqrt{\ln 2})/(\pi\Delta\nu)$ represents the coherence length of the Gaussian spectrum light source with a spectral bandwidth $\Delta\nu$ and c is the speed of light in vacuum. When the phase offset φ_0 is ignored, the term $4\pi(z-z_0)/\lambda_0$, which is called phase, can be used to determine the profile of a test object. For convenience, it is written as

$$\varphi = \frac{4\pi}{\lambda_0}(z-z_0) \quad (3)$$

In Eq. (3), the peak position z_0 of the coherence envelope indicates the height of a corresponding point on the test surface. In principle, when the vertical scanning position z equals z_0, the intensity of a white-light interference signal will be maximum. However, a recorded intensity peak may not indicate the actual position due to factors such as the discrete scanning of a piezoelectric transducer (PZT) and distortion or aberration of lenses in the system. However the recorded intensity peak position still can be used as an initial estimation. In the following discussion, we name a strategy as a direct peak detection (DPD) method which directly utilizes the recorded intensity peak position as the actual profile.

Due to its good ability to analyze fringe patterns in spatial-frequency domain [22–27], STFT can be used to accurately extract the recorded intensity peak position, estimate the center wavelength of the light source, and retrieve the corresponding phase value of the peak simultaneously. A STFT technique called

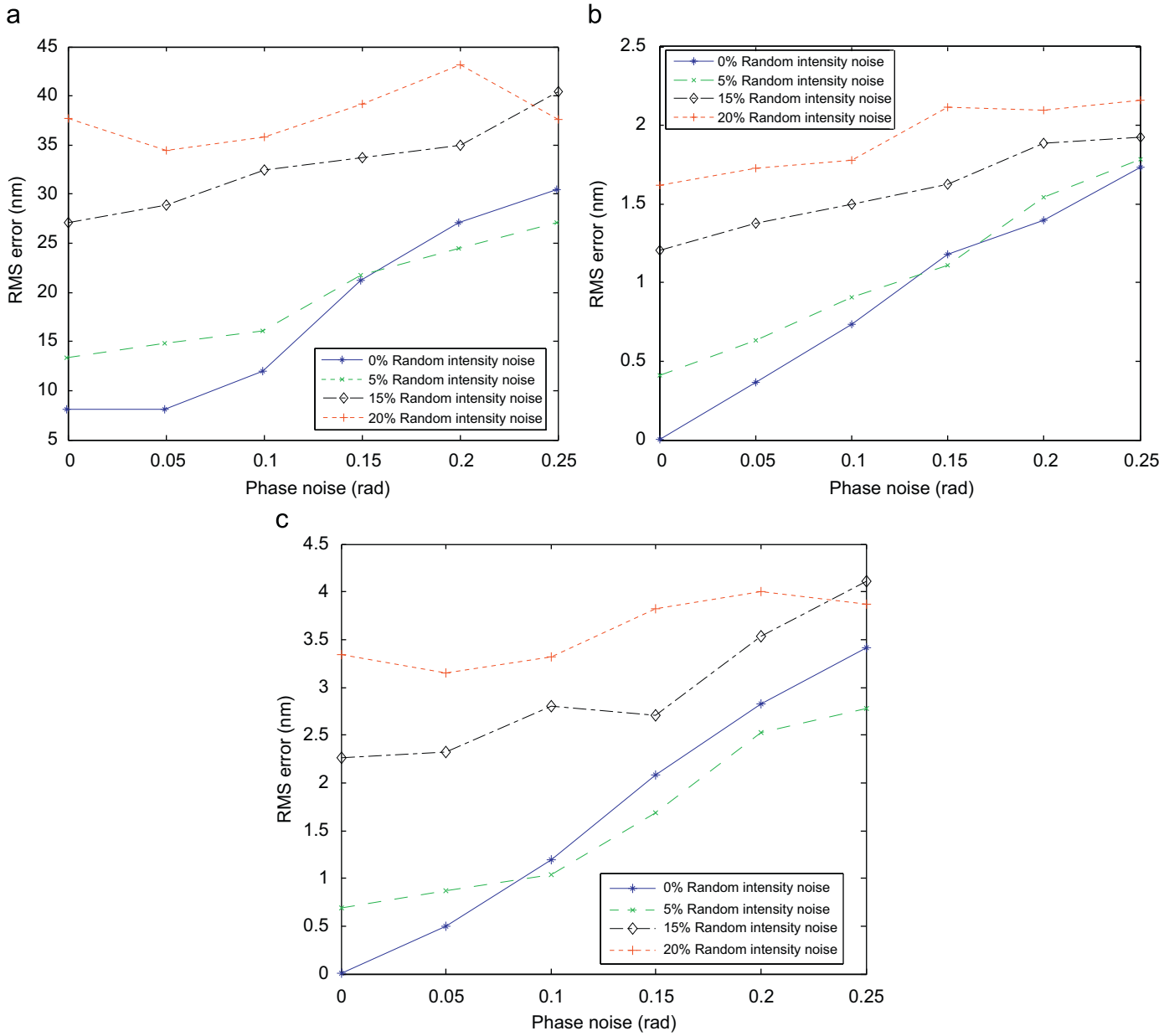

Fig. 2. Simulated results of an object with steps of 0.51 and 1.17 μm for various random intensities and phase noises. RMS error of (a) the profile obtained with the Direct Peak Detection method, (b) the profile obtained with the proposed method, and (c) the center wavelength obtained with the proposed method.

windowed Fourier filtering (WFF) [24,26] is utilized to accomplish the operations mentioned above. A complex filtered interference signal $\overline{I(z)}$, which is a best estimation on the original $I(z)$, is given by

$$\overline{I(z)} = \frac{1}{2\pi}\int_{-\infty}^{+\infty}\{[\overline{I(z)\otimes g(z,\xi)}]\otimes g(z,\xi)\}d\xi \tag{4}$$

where $g(z,\xi)=\exp(-z^2/2\sigma^2)\exp(j\xi z)$ is the kernel of the WFF, the parameter σ determines the window size of the WFF. Symbols $\otimes$ and $\overline{\ }$ indicate a convolution and filtering operation, respectively.

Since STFT is a correlation operation, when the highest similarity between an interference signal $I(z)$ and a kernel $g(z,\xi)$ occurs, the modulus of $\overline{I(z)}$ will also be the maximum, and the position of this maximal modulus can be used as the recorded intensity peak position.

2.2. Least-square estimation

In order to achieve a more accurate peak position of the coherence envelope, we propose a least-square estimation strategy using a line fitting. From Eq. (3), it can be seen that the equation is linear and can be further rewritten as

$$\varphi = Az + B \tag{5}$$

where $A=4\pi/\lambda_0$ is the slope, which contains a center wavelength information of the light source, and $B=-4\pi z_0/\lambda_0$ is the interception, which implies the profile information of a test object. When a phase φ is retrieved and the recorded peak intensity position is estimated by DPD method, with the least-square estimation, the profile of a test object can be determined accurately. It needs only several points (e.g. five points) near the recorded intensity peak position to accomplish the least-square estimation (based on Eq. (5)). Once the best approximation $\tilde{B}$ for B and the best approximation $\tilde{A}$ for A are obtained, the profile of a test object can be calculated as

$$z_0 = \frac{\tilde{B}\lambda_0}{(-4\pi)} = \frac{-\tilde{B}}{\tilde{A}} \tag{6}$$

and the center wavelength of a white-light source can be estimated as

$$\lambda_0 = \frac{4\pi}{\tilde{A}} \tag{7}$$

Furthermore, a complex phasor (CP) method [27] is introduced to further reduce the noise in phase values, which may have an influence on the least-square estimation mentioned above. When the CP method is used, an average filter is proposed to process the complex filtered interference signal ($\overline{I(z)}$). The average filter can be expressed as

$$\overline{I_{New}(z_m)} = \sum_{i=1}^{5}\mathrm{Re}[\overline{I(z_{mi})}]/5 + j*\sum_{i=1}^{5}\mathrm{Im}[\overline{I(z_{mi})}]/5 \tag{8}$$

where the summation is over 1×5 window centered at the given position z_m, $\overline{I_{New}(z_m)}$ is the processed signal. The phase values used in Eq. (5) are determined as

$$\varphi(z_m) = \mathrm{angle}[\overline{I_{New}(z_m)}] \tag{9}$$

Moreover, it is noteworthy that the scanning interval of PZT (Δz) should satisfy the following inequality [28] so as to avoid the spectral aliasing in the frequency domain when STFT is used for the peak detection and the phase values retrieval

$$\Delta z < \frac{\lambda_0}{4} \tag{10}$$

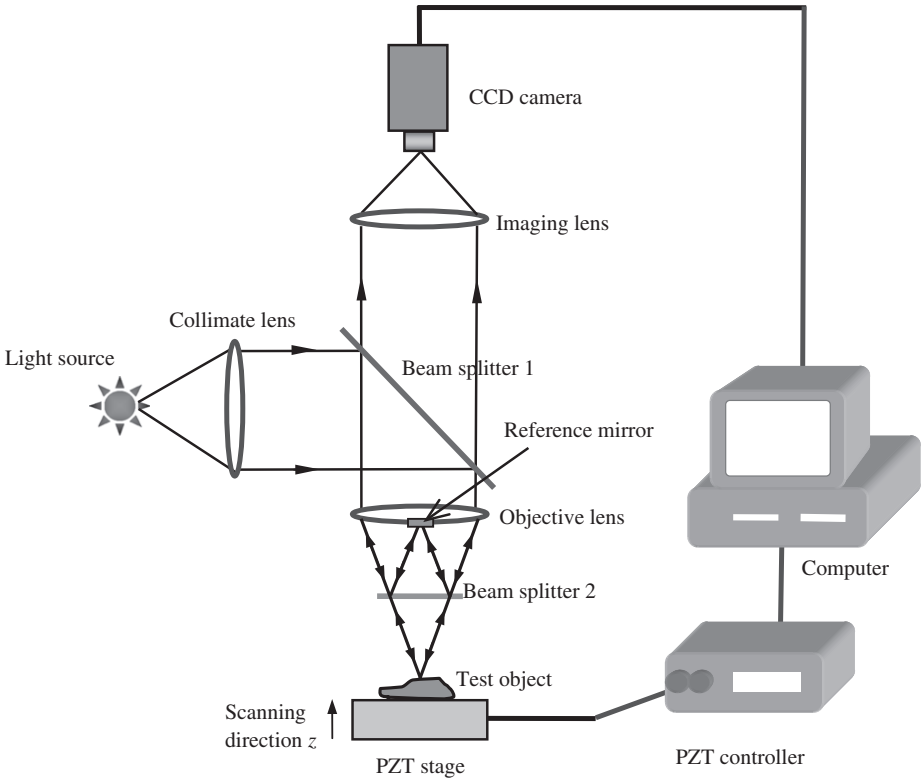

Fig. 3. Schematic experimental setup for Mirau-type WLSI.

3. Simulation

Fig. 1(a) shows a simulated white-light interference signal whose recorded intensity peak position is 5.55 μm. The maximum value position of modulus of the corresponding processed complex filtered interference signal ($\overline{I_{New}(z_m)}$) is also 5.55 μm, as shown in Fig. 1(b). Fig. 1(c) shows the five points around the recorded intensity peak position used in least-square estimation. It is seen that these points are linear, which verifies the validity of the proposed algorithm.

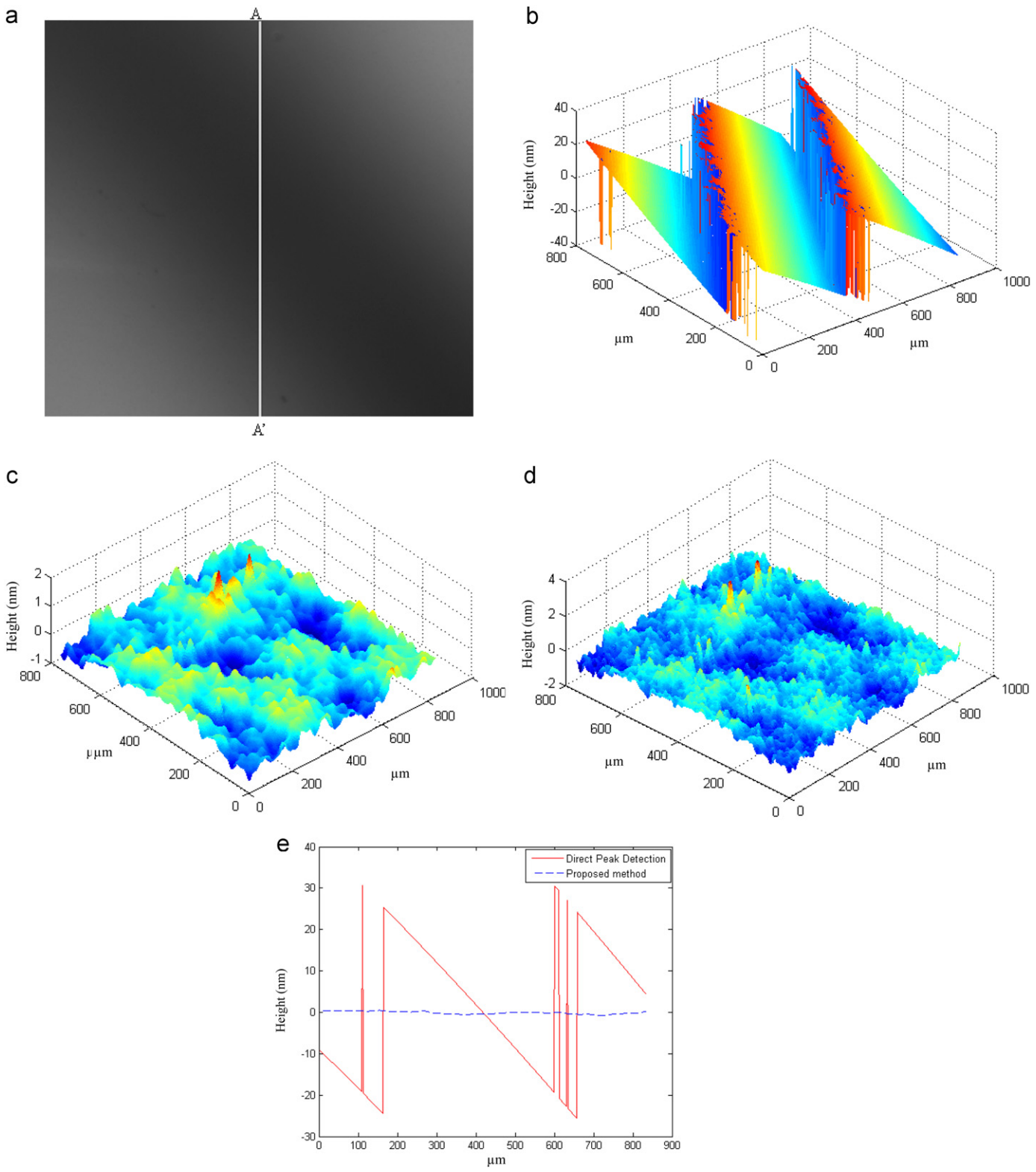

Fig. 4. Measured results of a standard flat mirror. (a) A white-light interference interferogram of a standard flat mirror. (b) Micro-profile of the mirror obtained with the Direct Peak Detection method. (c) Micro-profile of the mirror obtained with the proposed method. (d) Micro-profile of the mirror obtained with the SFD method. (e) Measurement along cross-section AA′ in (a).

Though the phase offset φ_0 is ignored in our proposed algorithm, as it is normally very small, it can still be considered as a phase noise. To study the effect of the phase offset φ_0 in our algorithm, a series of fringe patterns with various random intensities and phase noises were simulated. A test object (128×128 pixels) that contains two different step heights (0.51 and 1.17 μm) were used. The other parameters used in Eq. (2) are set as $I_0 = 100$, $\gamma = 80$, $l_c = 0.6$ μm, and $\lambda_0 = 0.56$ μm. A scanning interval of 0.05 μm and a scanning range of 0–10 μm were utilized. The random intensity noise level changes from 0% to 20% with a 5% increment. For the random phase noise, it changes from 0 to 0.25 rad with a 0.05 rad increment.

Fig. 2(a) shows the RMS error of the profile obtained with Direct Peak Detection (DPD) method. Fig. 2(b) shows the RMS error of the profile obtained with the proposed method. The RMS error of the center wavelength obtained with the proposed method is shown in Fig. 2(c). It is seen in Fig. 2(a) that using the DPD method for random intensity noise level below 15%, the random phase noise (between 0 and 0.25 rad) is the main factor that affects the RMS error. While, if the random intensity noise level increases to 15% and above, the intensity noise becomes the main factor. Similar characteristics are observed for the profile and center wavelength obtained using the proposed method (Fig. 2(b) and (c)). Comparing Fig. 2(a) with (b), it is found that the proposed algorithm has a better immunity to intensity and phase noises than the DPD method. The maximum RMS error (using least-square estimation) is no more than 2.5 nm. However, the corresponding value obtained with the DPD method is about 45 nm, which is 18 times larger than that of the proposed method. The maximum RMS error of the center wavelength obtained with the proposed method is less than 4.5 nm, as shown in Fig. 2(c). From the simulated results, it can be seen that ignoring the phase offset has little effect on the proposed algorithm.

4. Experiment and results discussion

Fig. 3 shows a schematic of the experimental setup. A halogen light source illuminates a test object through a collimating lens, a beam splitter (beam splitter 1), and a Mirau-type interference objective. Another beam splitter (beam splitter 2) and a reference mirror in the Mirau-type interference objective are incorporated to generate the reference and objective beams, which interfere with each other within the coherence length of the light source. The object is mounted on a PZT stage (PI-622.ZCD) controlled by a computer through a PZT controller (PI-E816.CR) to move along the scanning direction. A gray CCD camera (PULNiX TM-62EX) is used to capture and store a series of resulting fringe patterns during the scanning process.

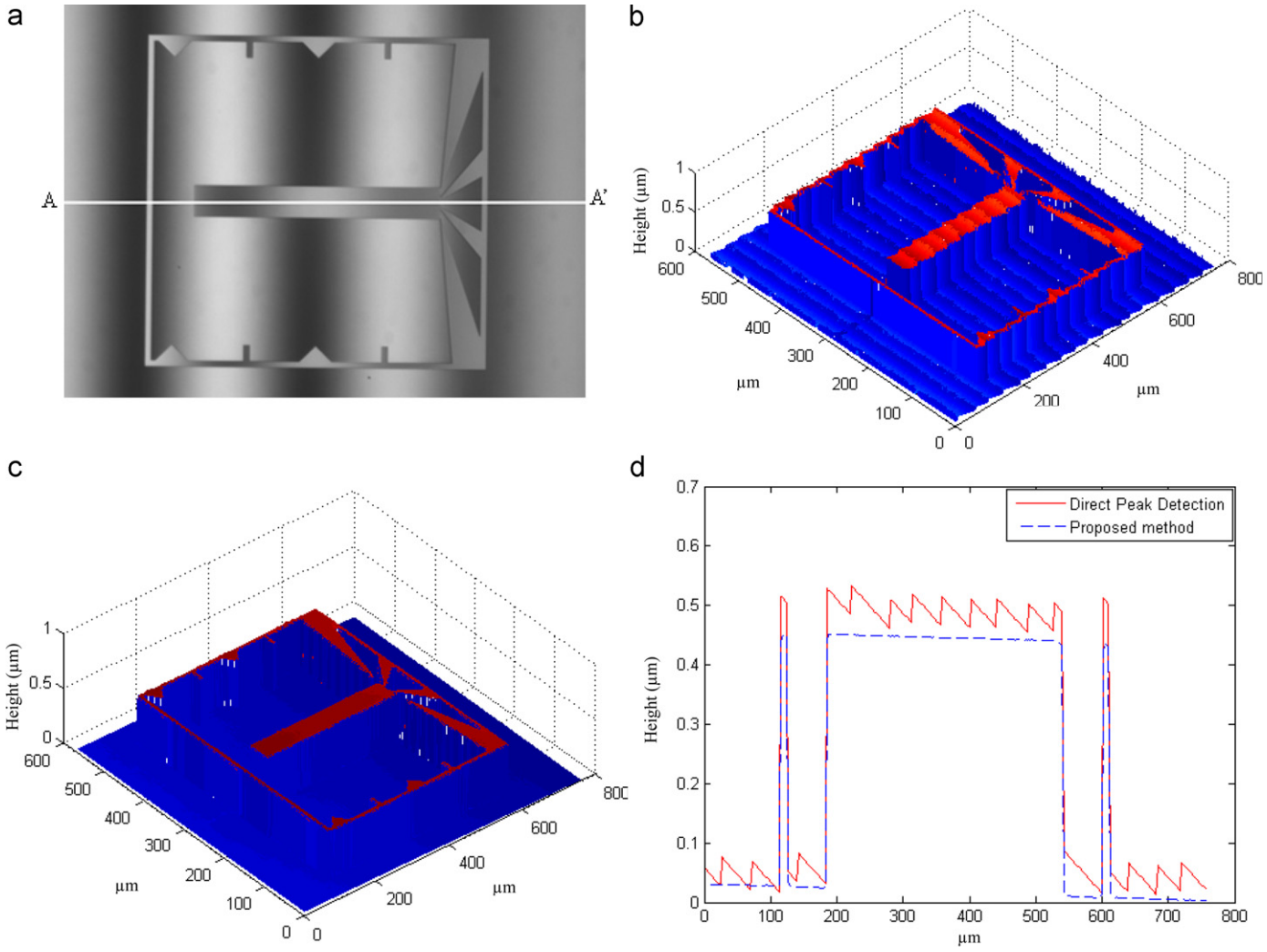

Fig. 5. Measured results of a micro-structure silicon wafer. (a) A white-light interference interferogram of a micro-structure silicon wafer. (b) Micro-profile of the object obtained with the Direct Peak Detection method. (c) Micro-profile of the object obtained with the proposed method. (d) Measurement along cross-section AA′ in (a).

A standard flat mirror, RMS of which is about 0.13 nm (specified by the manufacturer), is first measured to evaluate the proposed algorithm. Fig. 4(a) shows a white-light interferogram of the standard flat mirror. A 3D micro-profile measurement of the mirror using the DPD method is shown in Fig. 4(b). Fig. 4(c) shows a 3D micro-profile measurement using the proposed method. The 3D measurement results using the SFD method [19] are shown in Fig. 4(d) (with a RMS about 0.29 nm). The profile along a cross-section AA′ in Fig. 4(a) is shown in Fig. 4(d). It can be seen that there are conspicuous error steps (about 50 nm height) on the surface of the mirror, as shown in Fig. 4(b). The RMS of the mirror using the DPD method is 14.43 nm. However, using the proposed algorithm, the result of the mirror is no more than 2 nm, as shown in Fig. 4(c). The RMS is about 0.26 nm, which is consistent with the results of the SFD method (only a deviation of 0.03 nm) and is close to the specified value. Furthermore, it is much less (about 55 times) than that obtained with the DPD method as well. The validity of the proposed algorithm also can be seen in Fig. 4(e).

A micro-structure silicon wafer, the maximum height of which is 0.45 μm (specified by the manufacturer), is also measured using the proposed method. Fig. 5(a) shows a white-light interferogram of the micro-structure object. A 3D profile of the object measured with the DPD method is shown in Fig. 5(b). Fig. 5(c) shows a 3D profile measured with the proposed method. The profile along a cross-section AA′ in Fig. 5(a) is shown in Fig. 5(d). As shown in Fig. 5(b), there are obvious errors in the steps measured. The maximum height obtained with the DPD method is 0.5622 μm (an error of 24.9%). While, using the proposed method, a much better profile of the object is obtained, as shown in Fig. 5(c). The maximum height obtained with the proposed algorithm is 0.4557 μm, which only has a deviation of 5.7 nm and an error of 1.3% compared with the specified value. A comparison of the results between the DPD and the proposed method is shown in Fig. 5(d).

5. Concluding remarks

In this paper, a new algorithm, which is based on least-square estimation using STFT to measure the profile of a test object in WLSI, is described. The proposed algorithm utilizes a CP method to reduce the phase noise and improve the accuracy. The proposed method is simple and effective. Simulated results show that the described algorithm has good immunity to intensity and phase noises. Experiments on a standard flat mirror and a micro-structure silicon wafer have verified the validity of the algorithm.

References

[1] Sasaki O, Okazaki H. Sinusoidal phase modulating interferometry for surface profile measurement. Appl Opt 1986;25(18):3137–40.
[2] Caber PJ. Interferometric profiler for rough surfaces. Appl Opt 1993;32(19):3438–41.
[3] De Groot P, Biegen J, Clark J, De Lega XC, Grigg D. Optical interferometry for measurement of the geometric dimensions of industrial parts. Appl Opt 2002;41(19):3853–60.
[4] Wyant JC, Creath K. Advances in interferometric optical profiling. Int J Machine Tools Manuf 1992;32(1-2):5–10.
[5] Bhushan B, Wyant JC, Koliopoulos CL. Measurement of surface topography of magnetic tapes by Mirau interferometry. Appl Opt 1985;24(10):1489–97.
[6] Born M, Wolf E. Principles of optics. 6th ed.. Oxford: Pergamon; 1980.
[7] Patrick S, Gilbert T. Profilometry by zero-order interference fringe identification. J Modem Opt 1993;40(9):1691–700.
[8] Kino GS, Chim SSC. Mirau correlation microscope. Appl Opt 1990;29(26):3775–83.
[9] Chim SSC, Kino GS. Three-dimensional image realization in interference microscopy. Appl Opt 1992;31(14):2550–3.
[10] Park MC, Kim SW. Direct quadratic polynomial fitting for fringe peak detection of white light scanning interferograms. Opt Eng 2000;39(4):952–9.
[11] Chen S, Palmer AW, Grattan KTV, Meggitt BT. Digital signal-processing techniques for electronically scanned optical-fiber white-light interferometry. Appl Opt 1992;31(28):6003–10.
[12] Sandoz P. An algorithm for profilometry by white-light phase-shifting interferometry. J Mod Opt 1996;43(8):1545–54.
[13] Larkin KG. Efficient nonlinear algorithm for envelope detection in white light interferometry. J Opt Soc Am A 1996;13(4):832–43.
[14] Harasaki A, Schmit J, Wyant JC. Improved vertical-scanning interferometry. Appl Opt 2000;39(13):2107–15.
[15] Rolf-Jürgen R, Gunther N. Analysis of white-light interferograms using wavelet methods. Opt Commun 1998;148(1-3):122–8.
[16] Li M, Quan C, Tay CJ. Continuous wavelet transform for micro-component profile measurement using vertical scanning interferometry. Opt Lasers Technol 2008;40(7):920–9.
[17] Sarac Z. Analysis of white-light interferograms by using Stockwell transform. Opt Lasers Eng 2008;46(11):823–8.
[18] De Groot P, Deck L. Three-dimensional imaging by sub-Nyqusit sampling of white-light interferograms. Opt Lett 1993;18(17):1462–4.
[19] De Groot P, Deck L. Surface profiling by analysis of white-light interferograms in the spatial frequency domain. J. Mod Opt 1995;42(2):389–401.
[20] De Groot P. Methods and apparatus for surface topography measurement by spatial-frequency analysis of interferograms, 1995, US Patent 5398113.
[21] De Groot P, De Lega XC, Kramer J, Turzhitsky M. Determination of fringe order in white-light interference microscopy. Appl Opt 2002;41(22):4571–8.
[22] Quan C, Tay CJ, Chen H. Temporal phase retrieval from a complex field in digital holographic interferometry. Opt Lett 2007;32(12):1602–4.
[23] Quan C, Niu H, Tay CJ. An improved windowed Fourier transform for fringe demodulation. Opt Lasers Tech 2010;42(1):126–31.
[24] Qian K. Windowed Fourier transform for fringe pattern analysis. Appl Opt 2004;43(13):2695–702.
[25] Qian K, Wang H, Gao W. Windowed Fourier transform for fringe pattern analysis: theoretical analyses. Appl Opt 2008;47(29):5408–19.
[26] Zhong J, Zeng H. Multiscale windowed Fourier transform for phase extraction of fringe patterns. Appl Opt 2007;46(14):2670–5.
[27] Chen W, Quan C, Tay CJ. Retrieval of instantaneous frequency from digital holograms based on adaptive windows. Opt Eng 2008;47(6):065801-1-6.
[28] Ma S, Quan C, Zhu R, Tay CJ, Chen L, Gao Z. Micro-profile measurement based on windowed Fourier transform in white-light scanning interferometry. Opt Commun, accepted for publication.